



Contents lists available at ScienceDirect

Chinese Journal of Chemical Engineering

journal homepage: www.elsevier.com/locate/CJChE

Review

Flow-resistance analysis of nano-confined fluids inspired from liquid nano-lubrication: A review☆

Xianzhu Huang¹, Jian Wu^{1,2}, Yudan Zhu^{1,*}, Yumeng Zhang¹, Xin Feng¹, Xiaohua Lu^{1,*}¹ College of Chemical Engineering, State Key Laboratory of Materials-Oriented Chemical Engineering, Nanjing Tech University, Nanjing 210009, China² Division of Machine Elements, Luleå University of Technology, 97187 Luleå, Sweden

ARTICLE INFO

Article history:

Received 2 November 2016

Received in revised form 14 May 2017

Accepted 14 May 2017

Available online 1 July 2017

Keywords:

Flow resistance

Membrane separation

Liquid nano-lubrication

Model

Intermolecular interactions

AFM

ABSTRACT

How to reduce flow resistance of nano-confined fluids to achieve a high flux is a new challenge for modern chemical engineering applications, such as membrane separation and nanofluidic devices. Traditional models are inapplicable to explain the significant differences in the flow resistance of different liquid–solid systems. On the other hand, friction reduction in liquid nano-lubrication has received considerable attention during the past decades. Both fields are exposed to a common scientific issue regarding friction reduction during liquid–solid relative motion at nanoscale. A promising approach to control the flow resistance of nano-confined fluids is to reference the factors affecting liquid nano-lubrication. In this review, two concepts of the friction coefficient derived from fluid flow and tribology were discussed to reveal their intrinsic relations. Recent progress on low or ultra-low friction coefficients in liquid nano-lubrication was summarized based on two situations. Finally, a new strategy was introduced to study the friction coefficient based on analyzing the intermolecular interactions through an atomic force microscope (AFM), which is a cutting-point to build a new model to study flow-resistance at nanoscale.

© 2017 The Chemical Industry and Engineering Society of China, and Chemical Industry Press. All rights reserved.

1. Introduction

With the rapid development of nanoporous materials, modern chemical engineering processes involve micro–nano interfaces, such as nanoporous membranes for separation [1–3], nanomaterials for catalysis and adsorption [4] and nanofluidic devices [5–7]. Membrane separation provides various advantages, including energy saving and high efficiency. As such, this process has been widely applied to different fields, including water treatment, solvent recovery and product purification. For the membranes with large pore sizes (>10 nm), such as microfiltration and ultrafiltration, the related theoretical models for controlling the fluids to flow through the membranes have been well understood and used to develop membrane preparation techniques. However, the pore size of membranes for various processes *e.g.* nanofiltration, reverse osmosis and electrodialysis decreases to below several nanometres. Traditional macroscopic mass transfer models are inapplicable to explain the mechanism of selectively separating nano-confined molecules or ions, which greatly impedes the development

of such kind of membranes. It is known that membranes with very small pore size are essential for azeotrope system separation [8,9] and seawater desalination [10–12]. Meanwhile, anomalous phenomena *e.g.* ultraflux [13–16] and breaking-tradeoff [17–19] have also been observed in nano-confined membrane processes. Therefore, it is necessary to investigate the nano-confined mass-transfer models.

In essence, the nano-confined membrane separation is the process of overcoming liquid–liquid and liquid–solid resistance. Flow resistance reduction in nano-confined channels has also been widely explored [20]. Interfacial effects play an important role at nanoscale, and friction coefficient is considered as a dominant parameter because of high “surface-to-volume ratio” [21]. In this case, intermolecular forces including *steric* interactions/hydration, van der Waals interactions and *electrostatic* interactions [22] between wall and liquid molecules significantly contribute to flow resistance and thus cause these unique phenomena. Many possible mechanisms have been used to account for these phenomena, including appropriate strength of liquid–wall interaction and boundary slip [23–28] and breakdown of uniform fluid density [29–31]. Nair *et al.* [32] found a monolayer of water when water flowed through graphene-based membrane with passage between graphene sheets separated by 0.6–1.0 nm. Boundary slip remarkably affects flow resistance at nanoscale, which is influenced by major factors, including film thickness, contact angle [33], fluid–solid molecular interactions [34] and flow velocity and pressure [35].

Up to now, no suitable universal models have been proposed to describe the flow resistance of nano-confined fluids mainly because of

☆ Supported by the National Natural Science Foundation of China (21176112, 21576130, 21490584, 51005123), Qing Lan Project, the State Key Laboratory of Materials-Oriented Chemical Engineering (KL15-03), Specialized Research Fund for the Doctoral Program of Higher Education (20133221110001) and the Natural Science Foundation of Jiangsu Province (BK20130062).

* Corresponding authors.

E-mail addresses: ydzh@njtech.edu.cn (Y.D. Zhu), xhlu@njtech.edu.cn (X.H. Lu).

the lack of *in situ* characterization methods for molecular interaction forces. The similar problem has also been encountered in liquid nano-lubrication. To minimize energy loss, many efforts have been paid to obtain ultra-low friction coefficient. Reynolds [36] proposed lubrication theory (Fig. 1) that governs the differential fluid flow equation for a wedge-shaped film, and this theory is expressed as Reynolds equation. This theory is the basis of hydrodynamic lubrication (HDL) and elastohydrodynamic lubrication (EHL) [37]. Specifically speaking, Reynolds equation is derived from Navier–Stokes fluid flow equations, continuum equation or viscous flow laws and mass conservation, which are the basic principles of fluid flow (Fig. 1①). At nanoscale, building models by modifying macroscopic fluid flow theories makes slow progress (Fig. 1②). Given the fact that nanofluidics and liquid nano-lubrication are exposed to a common scientific issue regarding friction reduction during liquid–solid relative motion at nanoscale, a promising approach to control the flow resistance of nano-confined fluids is to reference the factors affecting liquid nano-lubrication. Inspired from liquid nano-lubrication insights by combining macroscopic lubrication theories and microscopic experimental tools, such as atomic force microscope (AFM), surface force balance (SFB) and surface force apparatus (SFA), to elucidate the factors influencing the flow of nano-confined fluids (Fig. 1③).

In the following sections, first, the two types of friction coefficient derived from fluid flow and tribology were discussed in detail, and the intrinsic relation was clarified. Second, recent developments focusing on low or ultra-low friction coefficient in two situations were reviewed in detail. Then, our recent progress of studying the friction coefficient based on analysing the intermolecular interactions *via* AFM was introduced and it could be considered as a cutting-point to build a new model to study flow-resistance at nanoscale. Finally, a brief conclusion and future perspective were provided.

2. Two Concepts of Friction Coefficient

Friction coefficient is an important parameter to characterize resistance in fluid flow and liquid lubrication. However, frequently used definitions of the friction coefficient in both fields are different, although they require a common physical model for liquid–solid relative motion.

The friction coefficient in nanofluidics is derived from the macroscopic fluid flow, whereas the friction coefficient in liquid nano-lubrication is derived from the macroscopic solid–solid tribology, as shown in Fig. 2.

2.1. Friction coefficient in fluid flow

Basing on continuous medium hypothesis, for the process of fluid flow around a sphere, the researcher [38] used the Navier–Stokes equation to describe the flow resistance and the friction coefficient as:

$$\zeta = 6\pi\eta d/m \quad (1)$$

where ζ is the friction coefficient of fluids flow around a sphere, η is the shear viscosity of the fluid, d is the diameter of the sphere and m is its mass. A more detailed investigation of the drag on a sphere is given by the Langevin equation [38] that describes the time-dependent drag on a rapidly oscillating sphere, shown in Eq. (2).

$$\frac{dv(t)}{dt} = - \int_0^t dt' \zeta(t-t')v(t') + \mathbf{F}_R(t) \quad (2)$$

where v is the velocity of fluid flow around sphere, \mathbf{F}_R is the random force per unit mass.

Since the early 19th century, researchers in fluid mechanics have studied the liquid–solid interface. In 1823, Navier described the existence of velocity difference called slip velocity between a fluid and a solid at the fluid–solid interface, which is also called the Navier partial slip boundary condition at the liquid–solid interface. Boundary slip means once the interfacial strength is insufficient to bear the large stress and then the fluid may slip on the contact surface with certain velocity difference. Thus, the slip velocity v_{slip} is linearly related to the slip length b and interfacial shear rate by [39,40]:

$$v_{\text{slip}} = b \left. \frac{\partial v}{\partial z} \right|_{\text{wall}} \quad (3)$$

where z is the coordinate along the normal to the wall. Many researchers [23,41] used slip length b to indicate the liquid–solid friction

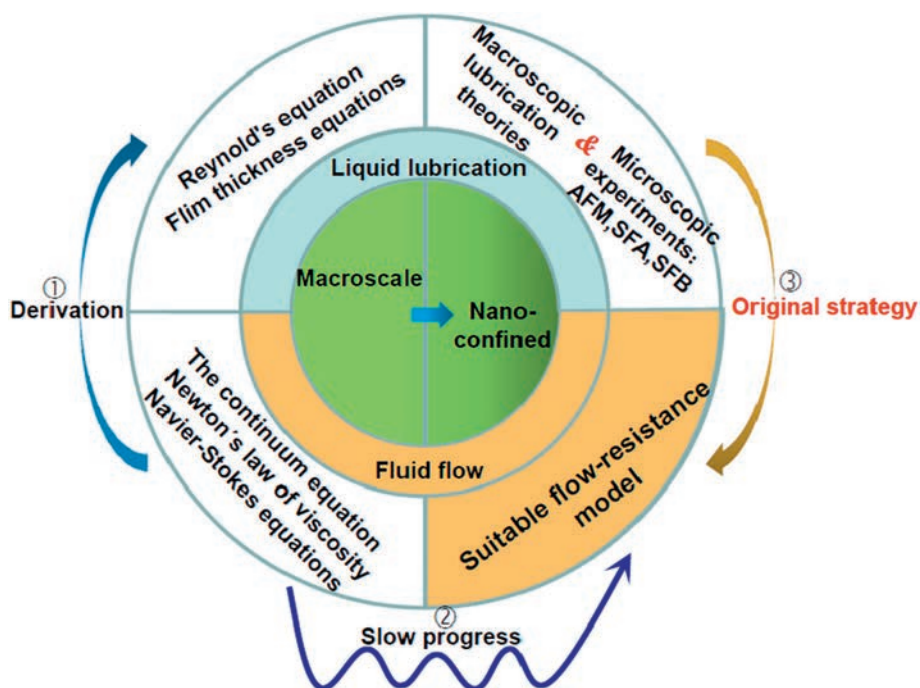


Fig. 1. Widely accepted theories in lubrication and fluid flow for macroscale and nanoscale. Relationship between liquid lubrication and fluid flow theories.

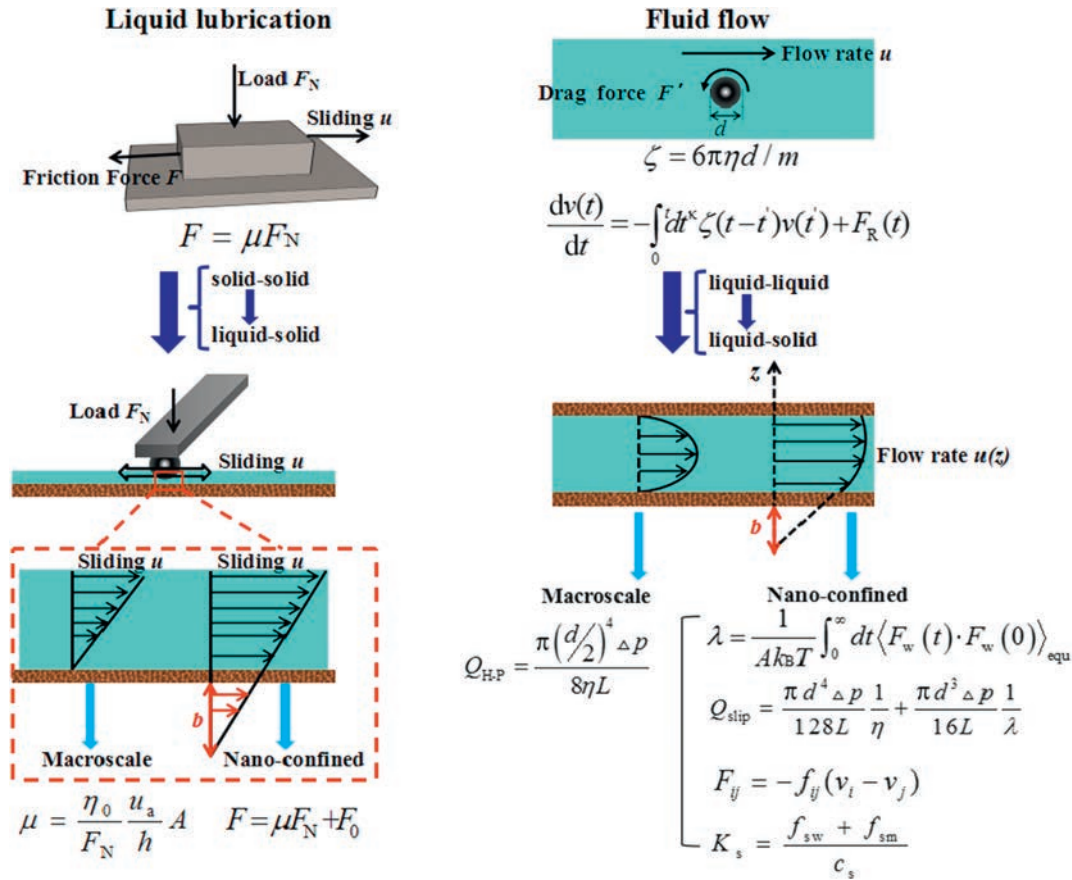


Fig. 2. Different definitions of solid-liquid friction coefficient at nanoscale derived from solid-solid motion (left) and liquid-liquid motion (right), respectively.

coefficient at the interface. The relationship between slip length b and friction coefficient λ is given by:

$$b = \eta / \lambda. \quad (4)$$

Furthermore, under the boundary slippage, an agreement that the friction force at the wall is linear to slip velocity v_{slip} [39] exists,

$$F_w = -A\lambda v_{\text{slip}} \quad (5)$$

where F_w is the total lateral force acting on the wall surface, λ is the liquid-solid friction coefficient and A is the lateral area.

To obtain an expression for the phenomenological friction coefficient, Bocquet *et al.* [42] proposed a derivation based on the Langevin approach for the Brownian motion of a massive wall in contact with a fluid in terms of equilibrium properties in the form of a Green-Kubo (GK) relationship [7,39,43]:

$$\lambda = \frac{1}{Ak_B T} \int_0^\infty dt \langle F_w(t) \cdot F_w(0) \rangle_{\text{equ}} \quad (6)$$

where T is the temperature, k_B is the Boltzmann constant, t is the time.

Falk *et al.* [44,45] used the definition of a liquid-solid friction coefficient, such as Eq. (6), to clarify fast liquid transport mechanisms in carbon nanotubes. The friction coefficient of water transport in carbon nanotube membranes exhibited strong curvature dependence and was found to vanish below a threshold diameter for armchair nanotubes. Furthermore, they proposed an approximate theoretical expression for the friction coefficient including curvature effect which fit well for different kinds of liquids (alcohols, alkanes and water).

For the flow in a circular pipe, the Hagen-Poiseuille equation with boundary slip [43,46], involves the relationship between flux and slip length b ,

$$Q_{\text{slip}} = \frac{\pi \left[\left(\frac{d}{2} \right)^4 + 4 \left(\frac{d}{2} \right)^3 b \right] \Delta p}{8\eta L} \quad (7)$$

where Q_{slip} is the volume flow rate with boundary slip, d is pipe diameter, L is pipe length, Δp is pressure differential and η is the viscosity of fluids. According to Eqs. (4) and (7), we could obtain the volume flow rate Q_{slip} as follows,

$$Q_{\text{slip}} = \frac{\pi d^4 \Delta p}{128L} \frac{1}{\eta} + \frac{\pi d^3 \Delta p}{16L} \frac{1}{\lambda} \quad (8)$$

From Eq. (8), Q_{slip} has strong dependence on the friction coefficient λ for a kind of fluid at the same condition. Namely, for a certain driving force, pipe diameter and length, fluid flow resistance is determined by the liquid viscosity and liquid-solid friction coefficient.

According to the thermodynamic principle [47], systems not far away from a global equilibrium may be extrapolated around an equilibrium state. For systems near equilibrium, linear phenomenological equations may represent the transport and rate processes. So, in a system near global equilibrium (system k), linear relations exist between flows J_i and thermodynamic driving forces X_k , the phenomenological equation is given by,

$$J_i = L_{ik} X_k \quad (9)$$

where the parameter L_{ik} is called the phenomenological coefficient of component i , which is related to transport coefficient. When analysing

membrane transport process, the phenomenological coefficient can be expressed in terms of the frictional force and a resistance-type phenomenological coefficient can be obtained [47]. For a solute in an aqueous solution, a steady-state flow is assumed and the thermodynamic forces \mathbf{X} are counterbalanced by a sum of suitable frictional forces \mathbf{F} . The force on the solute is described as:

$$\mathbf{X}_s = -\mathbf{F}_{sw} - \mathbf{F}_{sm} \quad (10)$$

where \mathbf{X}_s is the thermodynamic force of solute, \mathbf{F}_{sw} is the frictional force of solute applied by water, \mathbf{F}_{sm} is the frictional force of solute applied by membrane. Similarly, the force on water is expressed as:

$$\mathbf{X}_w = -\mathbf{F}_{ws} - \mathbf{F}_{wm} \quad (11)$$

where \mathbf{X}_w is the thermodynamic force of water, \mathbf{F}_{ws} is the frictional force of water applied by solute, \mathbf{F}_{wm} is the frictional force of water applied by membrane. In general, the individual friction forces \mathbf{F}_{ij} are assumed to be linearly proportional to the relative velocity:

$$\mathbf{F}_{ij} = -f_{ij}(v_i - v_j) \quad (12)$$

where \mathbf{F}_{ij} is the frictional force of component i applied by component j , f_{ij} is the frictional coefficient per mole of the component i , v_i is velocity of component i , v_j is velocity of component j .

Because the f_{ij} obeys the reciprocity relation, $c_i f_{ij} = c_j f_{ji}$ and the flows of solute \mathbf{J}_s and water \mathbf{J}_w can be expressed as $\mathbf{J}_s = c_s v_{s0}$, $\mathbf{J}_w = c_w v_{w0}$ respectively, where c_i is the concentration of specie i , c_j is the concentration of specie j , f_{ji} is the frictional coefficient per mole of the component j , we can express Eqs. (10) and (11) as,

$$\mathbf{X}_s = \frac{f_{sw} + f_{sm}}{c_s} \mathbf{J}_s - \frac{f_{sw}}{c_w} \mathbf{J}_w \quad (13)$$

$$\mathbf{X}_w = -\frac{f_{sw}}{c_w} \mathbf{J}_s + \frac{c_w f_{wm} + c_s f_{sw}}{(c_w)^2} \mathbf{J}_w \quad (14)$$

where the velocity of membrane is assumed as $v_m = 0$, c_s is the concentration of solute, c_w is the concentration of water. Eqs. (13) and (14) represent the resistance type of formulations, then the resistance phenomenological coefficient can be expressed as Eqs. (15) and (16),

$$K_s = \frac{f_{sw} + f_{sm}}{c_s} \quad (15)$$

$$K_w = \frac{c_w f_{wm} + c_s f_{sw}}{(c_w)^2} \quad (16)$$

where K_s is the resistance phenomenological coefficient between the solute and the membrane matrix, K_w is the resistance phenomenological coefficient between the water and the membrane matrix.

Compared with those in Eq. (5), the slip velocity v_s for component i is the relative velocity, $v_i - v_m$; therefore, f_{im} in Eq. (12) is related to friction coefficient λ . It is easy to find that K_s and K_w is related to friction coefficient λ . In sum, for membrane separation, high flux and selectivity can be obtained by adjusting the liquid–solid friction coefficient.

2.2. Friction coefficient in liquid lubrication

In general, the basic rule of intrinsic friction for solid–solid contact is described as Eq. (17) [37],

$$\mathbf{F} = \mu \mathbf{F}_N \quad (17)$$

where \mathbf{F} is the friction force, \mathbf{F}_N is the normal load and μ is the friction coefficient.

Sliding between solid surfaces is generally characterized by high friction coefficient and severe wear, whereas a thick liquid film sandwiched

between two solid surfaces in relative motion can prevent solid–solid contact and lead to low friction. The existence of laminar viscous flow is the key precondition for the original principle for macroscopic liquid lubrication. For concentric (lightly load) journal bearing, the friction force of Newtonian flow is given as [37],

$$\mathbf{F} = \eta_0 \frac{u_a}{h} A \quad (18)$$

where A is the surface area of the bearing interface, h is the film thickness, u_a is the relative velocity and η_0 is the viscosity at ambient pressure and constant temperature. According to Eq. (17), the friction coefficient for liquid lubrication can be given as follows:

$$\mu = \frac{\eta_0}{\mathbf{F}_N} \frac{u_a}{h} A \quad (19)$$

This equation is only valid for the lubrication regimes of HDL and EHL. Under boundary lubrication with film thickness of only several nanometres, any abnormal factors need to be considered (as mentioned above e.g. boundary slip and the breakdown of the uniform fluid density).

For viscous liquid at low applied loads or at nanoscale, the adhesion needs to be considered and the definition of friction coefficient is modified as [48,49]

$$\mathbf{F} = \mu \mathbf{F}_N + \mathbf{F}_0 \quad (20)$$

where μ and \mathbf{F}_0 are the slope and y-intercept, respectively. In most situations, μ is just the friction coefficient, and \mathbf{F}_0 is the force related to the chemical composition of the interface. The formula consists of (external) additive load-dependent and (internal) adhesion-dependent contributions. The adhesion contribution is proportional to the number of interatomic or intermolecular bonds that are broken and reformed when the surfaces slide laterally past each other [49]. Jiang *et al.* [50–54] used this equation to describe dynamic friction between two surfaces modified by self-assembled monolayers at nanoscale. First, they found that the friction coefficient for the OH/OH contact pair is much larger than those for the CH₃/CH₃ pair because of the formation of hydrogen bonds under dry sliding condition [50]. They also observed that the relative humidity (the number of water molecules) influenced hydrophilic monolayers but did not affect hydrophobic monolayers. As relative humidity increases, friction coefficient decreases quickly for hydrophilic monolayers [51]. Therefore, they investigated nanoscale friction of contact pair covered with alkyl monolayers lubricated with three solvents, and the friction coefficient calculated by using Eq. (20) was dependent on both surface hydrophobicity and solvent polarity.

Currently, many researchers studied boundary slip [55–57] and took advantage of slip to drastically reduce the friction, especially for severe EHL operating condition in industrial machinery [58,59] (or called thin-film lubrication) and lubricated micro/nanoelectromechanical systems (M/NEMS) [60] in which the film thickness is in the order of nanometre. A reduction of film thickness and weak interaction between wall and liquid favours the occurrence of interfacial slip. Under severe confinement, the internal cohesion of lubricants deviates from its bulk phase and significantly contributes to friction force [61]. The strength of interfacial interaction can be measured by contact angle, surface energy and spreading parameter. Huang *et al.* [62] found a quasiuniversal relationship between slip length and static contact angle. Meanwhile, Kalin *et al.* [63] considered a spreading parameter instead of the contact angle to be a reliable and relevant term for describing the wettability of surface. More appropriate parameters need to be proposed to quantify interfacial interaction. A quantitative analysis also existed besides the qualitative researches on the slip. These studies [35,64] integrated molecular-scale phenomena into macroscopic lubrication models based on the continuum hypothesis, namely, the Reynolds equation was modified to account for the occurrence of slip on the interface.

This was a multi-scale approach for a better understanding of the molecular effects on the global contact behaviour.

2.3. Essence: the lateral force of liquid–solid relative motion under nano-confinement

From Fig. 2, the two models showed clearly the different expressions of friction coefficient to describe the liquid–solid relative motion at nanoscale. Reconsidering the behaviour of the two movement models, in liquid-lubricated tribology, when the driving force is directionally applied on solid walls, the movement of liquid lubricant along with the wall is due to the liquid viscosity and liquid–solid interactions. Thus, the liquid resists the motion of the wall, which is named as lateral force or friction force F . For this reason, in this field, the friction coefficient μ is a measurement of the lateral force F acting on wall surface from liquid lubricant. By contrast, in fluid flow, driving force is directionally applied on fluids. Similarly, the solid wall surface has resistance on the flow of liquid for the liquid viscosity and liquid–solid interactions, which is named as lateral force or drag force F' . That is to say, in nanofluidics, the friction coefficient λ is a measurement of the lateral force F' acting on fluid from wall surface. Given the whole movement between liquid and solid, it is easily noted that the relationship of F and F' is the action and reaction. Based on Newton's third law, the values of F and F' are undoubtedly equal [23].

From the analysis of above, although the different origins and expressions of friction coefficient are for the two fields, their intrinsic relation is a measurement of lateral force during the liquid–solid relative motion. By dissecting this, a new insight from liquid nano-lubrication to consider flow-resistance under nano-confinement can be proposed. Liquid nano-lubrication focusing on low or ultra-low friction coefficient has made groundbreaking advances in both theories and experiments. It will be an avenue to combine microscopic frictional experiments and lubrication theories for analysing flowing resistance at nanoscale, which possesses potential in overcoming the difficulty for direct measurement of dynamic resistance. Thus, in the following, we reviewed the progress of achieving low or ultra-low friction coefficient on two situations in liquid nano-lubrication to obtain some useful understanding on flow-resistance minimization, which is a learning point for illustrating the transport mechanism of nano-confined fluids.

3. Progress of Achieving Low or Ultra-low Friction Coefficient in Liquid Nano-lubrication

For liquid lubrication, tribological systems with low or ultra-low friction coefficient need to be explored for the miniaturization of the high-tech mechanical equipment and minimum energy loss. However, because of different working conditions (e.g. applied load, sliding velocity, and temperature), materials of frictional pairs and lubricants in various areas are different and their methods of friction reduction also have their own features. In this part, we divided the works on achieving low friction coefficient at nanoscale into two kinds based on the liquid existence between solid surfaces. The first is that the liquid cannot separate the solid effectively in conditions like under high applied load or the liquid viscosity is too low. In this situation, the liquid is easy to be squeezed out and the solid surfaces come into contact directly. The typical fields include lubrication of synovial joints and M/NEMS. The other one is that the load is not so high and the solid surfaces are separated easily by the liquid. The behaviour of liquid transfers between solid surfaces is parallel to the liquid flow in membrane separation. In this situation, the friction coefficient origins from the viscous force of liquid and the slip resistance at the liquid–solid interfaces. In recent years a lot of achievements were gained in friction reduction in these two situations. For the first situation, the main method is to reinforce interfacial strength thus avoiding the direct solid contact. As for the second situation, on the contrary, the effort is on weakening the interfacial strength. In the following part, the recent works on these two situations will be analysed in detail.

3.1. Friction reduction by reinforcing interfacial strength

3.1.1. Hydration lubrication

One of the main methods is to strengthen hydration lubrication. Ions in aqueous solution, charged or polar macromolecule or polymer brushes possess stronger hydration strength to sustain high load without water being squeezed out [65]. The robust hydration shells acting as lubricating elements in boundary layer is the feature of hydration lubrication [66]. Raviv *et al.* [67] experimentally observed the fluidity of bound water molecules by SFB to demonstrate the reasonability of hydration lubrication. They found that the confined water film was only (1.0 ± 0.3) nm thick, whereas these highly compressed water molecules retained the shear fluidity of the bulk phase, which could be attributed to the ready exchange of water molecules within the hydration layers. In synovial joints with friction coefficient of 0.001, hyaluronan complexing with phosphatidylcholines at the cartilage surface provides hydration layer due to the exposed phosphocholine groups can be strongly hydrated [68]. Some surfaces coated with hydrophilic or charged polymer brusher in ionic aqueous solution lubrication can also achieve low or ultra-low friction coefficient under high load [69–71]. While hydrophobic coating [72] or ions with large ionic radius will lead to high friction since they cannot form hydration layers to bear load and separate the friction pairs.

Some acid or polyhydroxy alcohol solution can form hydrogen-bond networks (HBs) on the contact region and thus a fluid-hydrated water layer is fastened by the networks to bear load (liquid with low viscosity possessing poor load-capacity) [73–75]. To verify the existence of HBs, Yue *et al.* [73] elucidated the tribochemical mechanism of the silica/phosphoric acid system with low friction through reactive molecular dynamics simulations. They found that friction coefficient was closely associated with the number of interfacial hydrogen bonds. Moreover, the clustering and polymerisation of phosphoric acid molecules, as well as a considerable quantity of water molecules distributed mainly in the sliding interface, favour a lower friction coefficient (0.02) for $T = 1400$ K. Fig. 3 shows a schematic illustration of hydrogen-bonded networks.

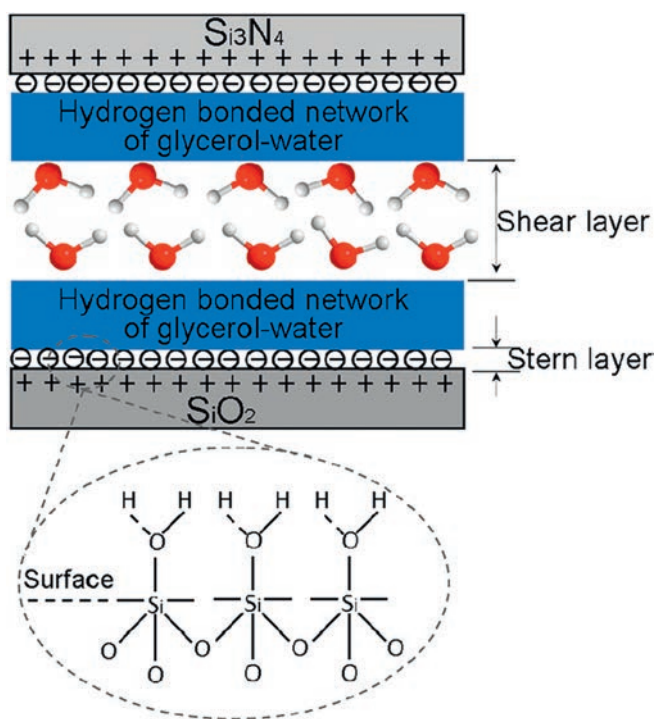


Fig. 3. Schematic illustration of hydrogen-bonded networks. Reprinted with permission from [76]. Copyright 2013 American Chemical Society.

3.1.2. Chemical reaction with the surface

Palacio *et al.* [77] found that ionic liquids (ILs) under different bonded conditions (untreated, partially bonded, fully bonded) exhibited distinct adhesive forces and friction coefficients. They deduced that a desirable combination of lubricant bonded to the substrate and a mobile fraction or appropriate solid–liquid interaction facilitated tip sliding. On the basis of these findings, Xue *et al.* [78,79] performed many explorations on dual-layer ultrathin films including stationary phase and mobile phase.

3.1.3. Electrical interaction

The surface electrical potential has a significant influence on the lubricity for ILs and the variety and orientation of the molecules near the surface are closely dependent on electrical potential [80], where they are anion enriched at the positive potentials and cation enriched at negative potentials. Molecular dynamics (MD) simulations [81] were adopted to theoretically elucidate the mechanism of the charge effect on the molecular ordering in the film. Under nano-confinement, two ways for energy dissipation existed. One is the rotation of dipoles and another is the slippages of the tip over potential barriers. Different potentials are needed for various ILs because of the different lubricity of the ions. However, using the same ILs as lubricants, the responses of friction reduction to the potential for different interfaces were different, which could be attributed to different liquid–solid interactions. For example, for the same ionic liquid lubricant, 1-hexyl-3-methylimidazolium tris (pentafluoroethyl) trifluorophosphate, the friction coefficient was 0.001 for +1.5 V at the SiO₂/(highly ordered pyrolytic graphite) interface [82], whereas the lowest friction coefficient was 0.1 for –2.0 V at the SiO₂/gold interface [80].

3.2. Friction reduction by weakening interfacial strength

According to hydration lubrication mechanism, in the lubrication of hydrated alkali metal ions, the order of lubricity should be $\text{Li}^+ > \text{Na}^+ > \text{K}^+$ due to the hydration strength ($\text{Li}^+ > \text{Na}^+ > \text{K}^+$). However, under the same condition, Gaisinskaya-Kipnis *et al.* [83] observed that the order of friction coefficient was $\text{Li}^+ > \text{Na}^+ > \text{K}^+$. It indicated that the higher hydration strength led to lower lubricity. Similarly controversy exists in nanofluidics. Hydrophobic surface or weak liquid–solid interaction promotes liquid slippage and the flow flux is enhanced [84]. While some reports also found an increased flux for hydrophilic surface or strong liquid–solid interaction [85–86]. It is important to figure out the working conditions of the frictional system. In Gaisinskaya-Kipnis's work, the solid surfaces can be separated by the solution and the slide needs to overcome the energy barriers of the hydrated ions. Strongly hydrated (and larger), surface-localized hydrated ions result in large energy barriers. This is one case that stronger interfacial strength results in higher friction. In fact, a lot of work has been done to study friction reduction by weakening the interfacial strength. Many possible mechanisms have been proposed, including boundary slip, layered structure of nanoconfined liquid, the reduction of hydrogen bonds, steric interactions/hydration, etc. The friction reduction according to the latter two mechanisms is just on the contrary to the methods in the Section 3.1.1. The mechanisms based on boundary slip and layered structure of nanoconfined liquid will be discussed.

3.2.1. Boundary slip

Normally, it is proposed that boundary slip is likely to be large on hydrophobic surfaces [84] and smaller or even zero on some hydrophilic surfaces [87]. However, it has been demonstrated that large slip can also occur on hydrophilic surfaces [33,88]. The hydrodynamic slip length was an intrinsic surface property, which was evaluated in nanochannels of varied sizes with different theories by Ramos-Alvarado *et al.* [89]. They successfully observed that the hydrodynamic slip length was channel-size independent for 5-nm channels or larger

by using equilibrium calculations while they failed to observe size effects for smallest channels (3 nm or lower).

Cieplak *et al.* [34] determined that the slip length was linked to the fluid organization near the solid, as governed by the fluid–solid molecular interactions, specifically in the second fluid layer normal to the wall. Fillot *et al.* [35,64] carried out a multiscale study on the wall slip effect in a ceramic–steel contact with nanometre-thick lubricant film by a nano-to-elastohydrodynamic lubrication approach. It provides a first insight on how an interface with two materials of different natures impacted film thickness and friction as slip occurred. In Fillot's work, slip dependence on the wall velocity, film thickness, and pressure is studied, and finally gets the multifactorial slip law.

3.2.2. Layered structure of nanoconfined fluid molecules

Nanoconfined fluid molecules is also very sensitive to the local chemical and physical environments, forming a regular shaped nanostream that has extremely low transport viscosity [90]. Numerous studies based on molecular dynamics (MD) simulations identified the breakdown of the uniform fluid density (layered structure of nanoconfined water) [91–93].

Neek-Amal *et al.* [94] found that the viscosity of water greatly varied because of the relationship between capillary size and water molecule size, and the flow rate of water was mainly affected by the layered structure of confined water with a separation of less than 2 nm. The results showed that smaller capillaries could enhance the shear viscosity and exhibited strongly related to the commensurability between the capillary size and the size of water molecules. Incommensurate relationship between capillary size and water molecule size will lead to sharply increased shear viscosity (shown in Fig. 4). So, studying slip length and flux rate should take the molecular structure of liquid and the subnanometer changes in the channel size in consideration.

Li *et al.* [95] directly measured the viscosity of the water film confined between the tip and surfaces when tip–surface distances were at $(0 \pm 0.03) \text{ nm} < d < 2 \text{ nm}$ by detecting simultaneously the normal solvation forces and the viscous lateral forces as a function of the tip to sample distance. The results showed that water at hydrophilic surface had a greater lateral force than hydrophobic surface because the orders of magnitude increased the viscosity. Layered water could be seen near hydrophilic surface.

Renou *et al.* [96] found a giant increase in the dielectric permittivity (“superpermittivity”) of liquids confined in CNTs, which was thought related to excluded volume effects inducing a preferential orientation of molecules. Watkins and Reischl [97] proposed a simple model to describe the tip force from water density, and used non-contact AFM experiments to quantitatively probe solvation structure in a non-invasive manner. They took a single water molecule as the tip model and calculate the change in free energy as it approached the surface over different lateral positions (the simulation way is proposed in their work [98]).

4. Progress in Analysing Flow-resistance of Nano-confined Fluids

Apparently, liquid nano-lubrication has many common mechanisms with fluid flow under nanoconfinement. The friction reduction based on the aforementioned mechanisms provides a guidance to lower the liquid flow resistance. However, to predict the flow resistance under nanoconfinement, the friction coefficient caused by liquid–solid interaction and liquid–liquid interaction (or viscosity) needs to be quantitatively measured. In the following sections, we summarize common methods for probing the behaviour of nano-confined fluids. Then, we emphasise AFM as an effective method for analysing flow resistance and introduce the related progress based on our recent investigations.

4.1. Common methods for probing behaviours of nano-confined fluids

MD simulation is necessary to investigate the static (structural) and dynamic properties of nano-confined fluids. MD simulation can be

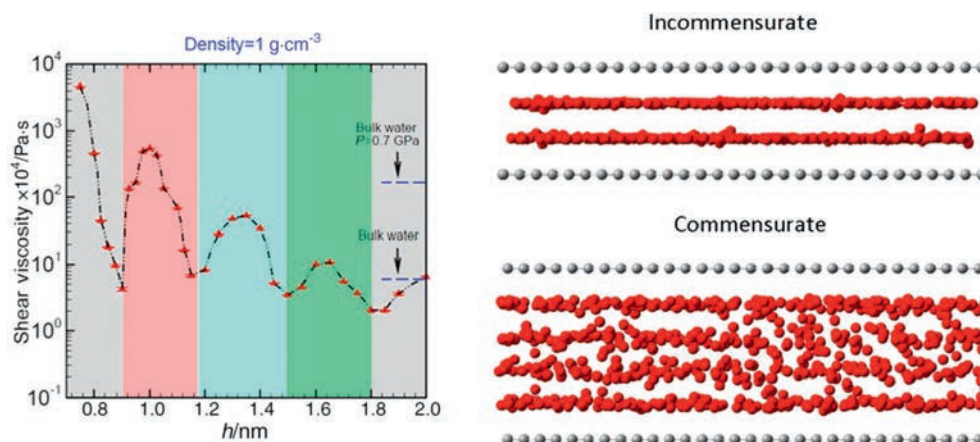


Fig. 4. (Left) the shear viscosity of confined water changes with the distance h separated between two graphene layers. (Right) Incommensurate and commensurate panel show the results corresponding to the maxima and minima of the shear viscosity shown in the left, respectively. Reprinted with permission from [94]. Copyright 2016 American Chemical Society.

helpful to obtain additional molecule-scale information and theoretically elaborate the mechanism of nano-confined fluid flow. Representative reviews have focused on the atomistic simulation of the behaviour of nano-confined fluids [22,99]. In liquid nano-lubrication, Vanossi *et al.* [100] reviewed some recent developments in modelling and atomistic simulation of friction. They pointed that MD simulation was good and informative for qualitative description of friction at nanoscale, but the simulation size and time limitations make it difficult to quantitatively compare with existing experimental results. In nanofluidics, our research group focused on the molecular simulation studies of nano-confined fluid molecule behaviour orienting toward nanoporous design and applications since the year 2000. We reviewed selected related works on molecular simulation of water molecules and ionic aqueous solution behaviour under nano-confinement and discussed some unsolved problems in simulations [101,102]. Recently, Hassan *et al.* [99] also pointed out the problem of time and spatial scale difference in simulations and the practical experiment process in their review of recent theoretical results about water inside carbon nanotubes using MD simulation, and suggested that several MD simulation parameters needed to be optimized to reflect recent experimental evidence. The development of experimental characterization techniques probing behaviour of nano-confined fluids is essential to verify the simulation results; however, the challenges are increased when the systems shrink to nanoscale.

We summarized the main experimental methods for probing the behaviour of nano-confined fluids in Table 1, for both nanofluidics and liquid nano-lubrication. The methods can be divided into two types. One probes the static (structural) properties and another detects the relative directed motion of fluids (lubrication). The characterizations of the static (structural) properties in nanofluidics and liquid nano-lubrication are universal, and the fluidic structure under nano-confinement can be experimentally probed [74,103,104]. X-ray, neutron diffraction, X-ray absorption spectroscopy (XAS) and X-ray Raman scattering (XRS) are the workhorses for the determination of nano-confined fluidic structure [105–109]. A large part of this structure always depends on the time scale. Time-resolved infrared spectroscopy, transmission electron

microscopy (TEM), and ultrafast electron diffraction (UED) [110–113] provided powerful high spatial and temporal resolution tools to determine this variability. Given the large specific surface area at nanoscale, the fluidic structure is significantly influenced by the surface structure and chemical composition of materials. To discover the structure and chemical composition of nanopores wall, attenuated total reflection Fourier-transform infrared spectroscopy (ATR-FTIR), nuclear magnetic resonance (NMR), X-ray photoelectron spectroscopy (XPS) and Rutherford backscattering spectrometry (RBS) can be used [114–117]. Holt [103] reviewed some experimental techniques for probing water at the nanoscale and more detailed information can be obtained.

To understand flow-resistance properties of nano-confined fluids, the detection of relative directed motion behaviour is required. On the one hand, in nanofluidics, experimental methods in existence cannot be used for analysing flow resistance of relative motion between fluids and wall surface. For membrane separation, using Eq. (7) to calculate volumetric flow rate is an indirect method to measure the value of flow resistance [118], while *in situ* detecting the flow resistance is vital for modelling flow-resistance at nanoscale. On the other hand, in liquid nano-lubrication, many experimental technologies are effective methods for obtaining information about flow resistance of nano-confined fluids. AFM, SFB, SFA and quartz crystal microbalance (QCM) are widely used in nanotribological and nanomechanics studies. SFA can measure the normal and lateral forces between two molecularly smooth mica surfaces lubricated with thin liquid film, and the thickness is well defined up to a resolution of 0.1 nm. Recently, we proposed an alternative avenue that continuously moving the pore walls could also direct the confined fluid flow, namely, the method adopted in liquid nano-lubrication. A primary exploration was taken to analyse the flow properties of the nano-confined water with MD simulations by Zhu *et al.* [119]. We concluded the flow resistance of confined water molecules mainly from the friction between water and wall interactions and the interactions among the water molecules themselves. The friction coefficient between the confined water and the pore wall increased with the hydrophilicity of pore walls. Moreover, further hydrophilicity results in changes of water orientation adjacent to wall surface and more hydrogen bonds between the water layers, which in turn enhanced the flow resistance originating from the water molecules themselves. In the following section, we introduce an exploration with AFM for describing flow resistance of nano-confined fluids based on intermolecular interactions.

4.2. Flow resistance analysis of nano-confined fluids based on AFM

Conventionally, AFM is a powerful tool to gain surface morphology and roughness information with nanometre resolution and can obtain

Table 1
Main experimental methods for probing the behaviour of nano-confined fluids

	Structural properties	Behaviour of the relative directed motion
Liquid nano-lubrication	X-ray, neutron diffraction XPS, XAS, TEM, UED, etc.	AFM, SFA, SFB, QCM, etc. used to analyse flow resistance via getting b and friction coefficient
Nanofluidics		Lack of effective methods <i>in situ</i> characterize flow resistance

a high-resolution image of the materials' three-dimensional surface microstructure *via* weak interaction force between the tip and measured sample. Given the relative motion between the tip and sample in detection process, AFM is a promising tool to analyse flow resistance of nano-confined fluid molecules. Our group performed preliminary explorations on it and two main contributions of AFM in flow-resistance analysis.

AFM can quantitatively obtain information about flow resistance of nano-confined fluids such as slip length, viscosity and friction coefficient. The occurrence of interfacial slip has the potential to affect the physics of flow in nano-confinement. Zhu *et al.* [120–122] reported studies on boundary slip for the flow of a simple liquid in a confined geometry obtained by measuring hydrodynamic drainage forces with AFM and proved that the measurement of the slip length b was reproducible. Further, AFM can detect the lateral force suffered by nano-scale fluidic molecules. The normal solvation forces and the viscous lateral forces of water under subnanometer confinement can be directly detected [95]. An *et al.* [123] found that the roughness of mesoporous TiO_2 films was ten times higher than densely packed TiO_2 films, while friction coefficient decreased 12-fold. When the tip approaches the surface of TiO_2 films, it comes in contact with water molecules around the TiO_2 surface instead of direct contact with TiO_2 films. Given the different roughness of mesoporous and dense TiO_2 films, the tip comes into contact with different water layers adsorbed on the TiO_2 films, as shown in Fig. 5. The suggested mobility of water layers was different. This could

be validated by the finding of Zhu *et al.* [124]. They observed that the water adsorbed on the surface of titanium dioxide nanoparticles had three different layers by using ^1H solid-state nuclear magnetic resonance. The innermost layer is highly immobilised water that is strongly confined on the surface of TiO_2 nanoparticles and the outermost layer is mobile water.

AFM can measure the difference of friction coefficient resulting from interactions between water and wall and the interactions among the water molecules themselves at nanoscale. Further, building a quantitative relationship between friction coefficient and intermolecular interactions helps to model flow resistance of nano-confined fluids. Gubbins *et al.* [125] found that the wetting behaviour of the liquid was determined by the strength of liquid–liquid and liquid–solid intermolecular interaction and the solid structure. They introduced the microscopic wetting parameter α_w to represent wetting, which reflected the relative value of liquid–solid to liquid–liquid interaction, as shown in Fig. 6. This parameter emerged naturally from a corresponding state analysis of the partition function for the system and proved to be a monotonic function of the contact angle [126]. Basing on the analysis of α_w , and depending on the analysis of friction theory and a corresponding states theory, An *et al.* [127] found that the nano-friction coefficient was a function of the dimensionless parameter (termed as structure adhesion parameter β , $\beta = \rho_s \Delta_s \sigma_s^2$, ρ_s is the number density of solid atoms per unit volume (unit: m^{-3}), Δ_s is the distance between two successive lattice planes of

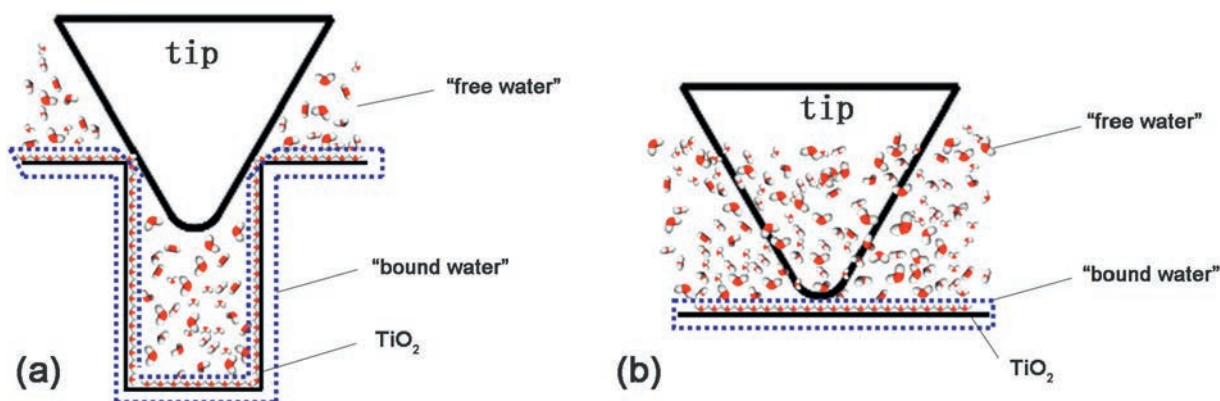


Fig. 5. Illustrations of AFM tip on (a) the mesoporous and (b) the dense TiO_2 film surfaces in the presence of water molecules. Reprinted with permission from [123]. Copyright 2012 American Chemical Society.

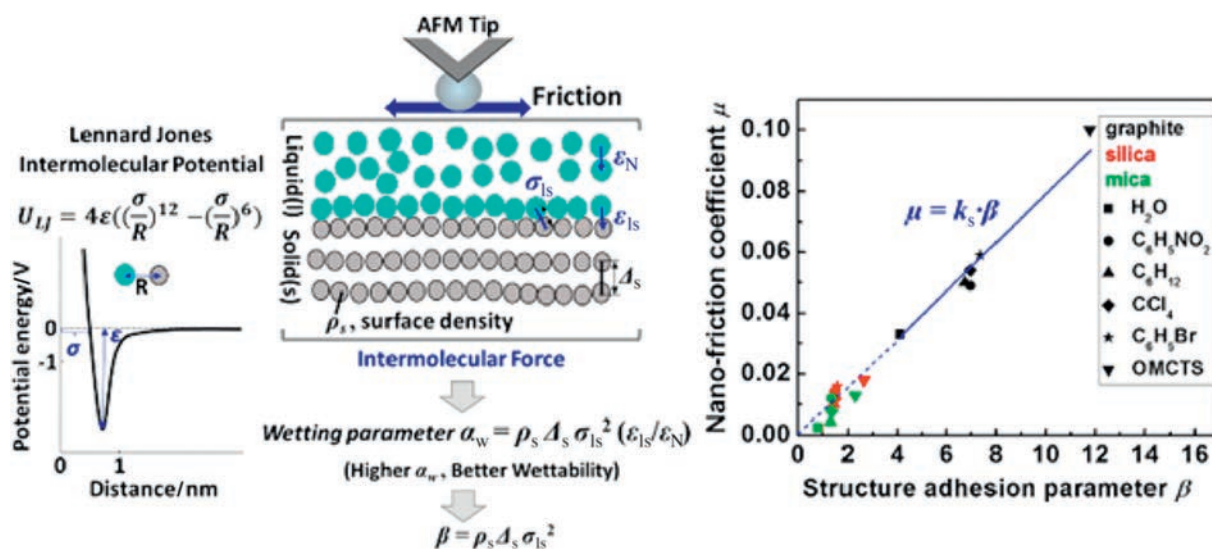


Fig. 6. Quantitative linear relationship between the structure adhesion parameter, β determined by the intermolecular parameters and liquid–solid nano-friction coefficient μ obtained from AFM experimental measurements. Reprinted with permission from [127]. Copyright 2016 American Chemical Society.

the substrate (unit: m) based on the assumption that the substrate atoms are arranged in layers, σ_{ls} is the molecular diameter that characterizes the liquid–substrate interaction (unit: m), shown in Fig. 6) reflecting the intermolecular forces involved and the structure of the solid substrate. An AFM experiment was performed and β was found to be linear with the nano-friction coefficient μ . As mentioned above, it is expected to potentially predict the resistance of liquid–solid systems under nano-confinement via calculation of structure adhesion parameter β .

5. Summary and Perspective

This review aims to provide an enlightening way to analyse flow resistance of nano-confined fluids derived from liquid nano-lubrication. Nanofluidics and liquid nano-lubrication are subjected to investigation of liquid–solid relative directed motion and have a common scientific question on lowering friction coefficient during liquid–solid relative movement at nanoscale. Two concepts of liquid–solid friction coefficient are discussed on the basis of fluid flow and tribology. It is found that their common essence is the lateral force that causes the resistance of liquid–solid relative motion during liquid–solid relative motion. As there have been a lot of efforts on liquid nano-lubrication, this review presents the recent progress on obtaining low or ultra-low friction coefficient. The mechanisms for two situations in liquid lubrication are discussed to shed lights on lowering flow resistance of nano-confined fluids. Although different mechanisms on friction coefficient reduction have been proposed, a quantitative analysis about interactions between liquids and wall surfaces or among lubricant molecules should be proposed. This review further summarizes the development in the analysis of flow resistance of nano-confined fluids and proposes a promising avenue in building a new model for flow-resistance research at nanoscale based on AFM.

Future studies should focus on systems used in nanofluidic or nano-confined separation through liquid nano-lubrication experiments, which are necessary to develop universal models that describe the relationship between friction coefficient and intermolecular interaction forces. However, friction coefficient obtained from liquid nano-lubrication cannot be directly used to calculate volume flow rate according to Eq. (8) for flux prediction. As such, a more accurate quantitative relevance of two kinds of friction coefficient should be investigated in detail.

Nomenclature

A	the lateral area
b	slip length
c_s	the concentration of solute
c_w	the concentration of water
d	the diameter of the sphere
EHL	elastohydrodynamic lubrication
F	friction force in tribology
F'	friction force in nanofluidics
F_{ij}	the frictional force between component i and j
F_N	the normal load
F_R	The random force per unit mass
F_{sm}	the frictional force of solute applied by membrane
F_{sw}	the frictional force of solute applied by water
F_w	the total lateral force acting on the wall surface
F_{wm}	the frictional force of water applied by membrane
F_{ws}	the frictional force of water applied by solute
F_0	y-intercepts
f_{ij}	the frictional coefficient per mole of the component i
HDL	hydrodynamic lubrication
h	the film thickness
J_i	flows of component i
J_s	flows of solute
J_w	flows of water

K_s	resistance phenomenological coefficient between the solute and membrane matrix
K_w	resistance phenomenological coefficient between the water and membrane matrix
L_{ik}	the phenomenological coefficient of i component in the system k
m	the mass of the sphere
Q_{slip}	the volume flow rate with boundary slip
T	temperature
t	time
u_a	the relative velocity
X	thermodynamic forces
X_k	thermodynamic driving forces in the system k
X_m	thermodynamic force of water
X_s	thermodynamic force of solute
z	the coordinate along the normal to the wall
α_w	microscopic wetting parameter
β	structure adhesion parameter
η	viscosity of the fluid
η_0	the viscosity at ambient pressure and constant temperature
k_B	the Boltzmann constant
λ	friction coefficient in nanofluidics
μ	the friction coefficient in tribology
v	the velocity of fluids flow around sphere
v_i	velocity of component i
v_j	velocity of component j
v_w	velocity of water
v_{slip}	slip velocity
v_{so}	velocity of solute
ζ	friction coefficient of fluids flow around a sphere

References

- [1] S.K. Bhatia, D. Nicholson, Modeling mixture transport at the nanoscale: Departure from existing paradigms, *Phys. Rev. Lett.* 100 (23) (2008) 236103.
- [2] D.C. Tanugi, J.C. Grossman, Water desalination across nanoporous graphene, *Nano Lett.* 12 (7) (2012) 3602–3608.
- [3] S.K. Bhatia, Modeling pure gas permeation in nanoporous materials and membranes, *Langmuir* 26 (11) (2010) 8373–8385.
- [4] S.K. Bhatia, M.R. Bonilla, D. Nicholson, Molecular transport in nanopores: A theoretical perspective, *Phys. Chem. Chem. Phys.* 13 (34) (2011) 15350–15383.
- [5] W. Sparreboom, A.V.D. Berg, J.C.T. Eijkel, Transport in nanofluidic systems: A review of theory and applications, *New J. Phys.* 12 (1) (2010) 015004.
- [6] J.C.T. Eijkel, A.V.D. Berg, Nanofluidics: What is it and what can we expect from it, *Microfluid. Nanofluid.* 1 (3) (2005) 249–267.
- [7] L. Bocquet, E. Charlaix, Nanofluidics, from bulk to interfaces, *Chem. Soc. Rev.* 39 (3) (2010) 1073–1095.
- [8] R.P. Pandey, V.K. Shahi, Functionalized silica–chitosan hybrid membrane for dehydration of ethanol/water azeotrope: Effect of cross-linking on structure and performance, *J. Membr. Sci.* 444 (2013) 116–126.
- [9] L. Vane, V. Namboodiri, G. Lin, M. Abar, F. Alvarez, Preparation of water-selective polybutadiene membranes and their use in drying alcohols by pervaporation and vapor permeation technologies, *ACS Sustain. Chem. Eng.* 4 (8) (2016) 4442–4450.
- [10] X. Tong, B.P. Zhang, Y.S. Chen, Fouling resistant nanocomposite cation exchange membrane with enhanced power generation for reverse electrodialysis, *J. Membr. Sci.* 516 (2016) 162–171.
- [11] J. Liu, J.S. Yuan, Z.Y. Ji, B.J. Wang, Y.C. Hao, X.F. Guo, Concentrating brine from seawater desalination process by nanofiltration–electrodialysis integrated membrane technology, *Desalination* 390 (2016) 53–61.
- [12] R.C. Rollings, A.T. Kuan, J.A. Golovchenko, Ion selectivity of graphene nanopores, *Nat. Commun.* 7 (2016) 11408.
- [13] J.K. Holt, H.K. Park, Y.M. Wang, M. Stadermann, A.B. Artyukhin, C.P. Grigoropoulos, A. Noy, O. Bakajin, Fast mass transport through sub-2-nanometer carbon nanotubes, *Science* 3 (12) (2006) 1034–1037.
- [14] A. Ghofri, A. Szymczyk, P. Malfreyt, Ultrafast diffusion of ionic liquids confined in carbon nanotubes, *Sci. Rep.* 6 (2016) 28518.
- [15] R.H. Tunuguntla, F.I. Allen, K. Kim, A. Belliveau, A. Noy, Ultrafast proton transport in sub-1-nm diameter carbon nanotube porins, *Nat. Nanotechnol.* 11 (7) (2016) 639–644.
- [16] A. Akbari, P. Sheath, S.T. Martin, D.B. Shinde, M. Shaibani, P.C. Banerjee, R. Tkacz, D. Bhattacharyya, M. Majumder, Large-area graphene-based nanofiltration membranes by shear alignment of discotic nematic liquid crystals of graphene oxide, *Nat. Commun.* 7 (2016) 10891.

- [17] H.W. Kim, H.W. Yoon, S.M. Yoon, B.M. Yoo, B.K. Ahn, Y.H. Cho, H.J. Shin, H. Yang, U. Paik, S. Kwon, J.Y. Choi, H.B. Park, Selective gas transport through few-layered graphene and graphene oxide membranes, *Science* 342 (6154) (2013) 91–95.
- [18] S.N. Yu, Z.Y. Jiang, S. Yang, H. Ding, B.F. Zhou, K. Gu, D. Yang, F.S. Pan, B.Y. Wang, S. Wang, X.Z. Cao, Highly swelling resistant membranes for model gasoline desulfurization, *J. Membr. Sci.* 514 (2016) 440–449.
- [19] J. Shen, G.P. Liu, K. Huang, Z.Y. Chu, W.Q. Jin, N.P. Xu, Subnanometer two-dimensional graphene oxide channels for ultrafast gas sieving, *ACS Nano* 10 (3) (2016) 3398–3409.
- [20] S.K. Bhatia, D. Nicholson, Friction between solids and adsorbed fluids is spatially distributed at the nanoscale, *Langmuir* 29 (47) (2013) 14519–14526.
- [21] S. Balasubramanian, C.J. Mundy, Calculation of friction coefficient of a solid-liquid interface via a non-equilibrium molecular dynamics simulation, *Bull. Mater. Sci.* 22 (5) (1999) 873–876.
- [22] H. Daiguji, Ion transport in nanofluidic channels, *Chem. Soc. Rev.* 39 (3) (2010) 901–911.
- [23] S. Nakaoka, Y. Yamaguchi, T. Omori, M. Kagawa, T. Nakajima, K. Fujimura, Molecular dynamics analysis of the velocity slip of a water and methanol liquid mixture, *Phys. Rev. E* 92 (2) (2015) 022402.
- [24] J.T. Cheng, N. Giordano, Fluid flow through nanometer-scale channels, *Phys. Rev. E* 65 (3) (2002) 031206.
- [25] V.P. Sokhan, D. Nicholson, N. Quirke, Fluid flow in nanopores: An examination of hydrodynamic boundary conditions, *J. Phys. Chem.* 115 (8) (2001) 3878–3887.
- [26] V.P. Sokhan, D. Nicholson, N. Quirke, Fluid flow in nanopores: Accurate boundary conditions for carbon nanotubes, *J. Chem. Phys.* 117 (18) (2002) 8531–8539.
- [27] Y.X. Zhu, S. Granick, Limits of the hydrodynamic no-slip boundary condition, *Phys. Rev. Lett.* 88 (10) (2002) 106102.
- [28] A. Waghe, J.C. Rasaiah, G. Hummer, Filling and emptying kinetics of carbon nanotubes in water, *J. Chem. Phys.* 117 (23) (2002) 10789–10795.
- [29] S. Joseph, N.R. Aluru, Why are carbon nanotubes fast transporters of water, *Nano Lett.* 8 (2) (2008) 452–458.
- [30] T. Ohba, K. Kaneko, M. Endo, K. Hata, H. Kanoh, Rapid water transportation through narrow one-dimensional channels by restricted hydrogen bonds, *Langmuir* 29 (4) (2013) 1077–1082.
- [31] C.L. Wang, B.H. Wen, Y.S. Tu, R.Z. Wan, H.P. Fang, Friction reduction at a superhydrophilic surface: Role of ordered water, *J. Phys. Chem. C* 119 (21) (2015) 11679–11684.
- [32] R.R. Nair, H.A. Wu, P.N. Jayaram, A.K. Geim, Unimpeded permeation of water through helium-leak-tight graphene-based membranes, *Science* 335 (6067) (2012) 442–444.
- [33] R.S. Voronov, D.V. Papavassiliou, L.L. Lee, Boundary slip and wetting properties of interfaces: Correlation of the contact angle with the slip length, *J. Chem. Phys.* 124 (20) (2006) 204701.
- [34] M. Cieplak, J. Koplik, J.R. Banavar, Boundary conditions at a fluid-solid interface, *Phys. Rev. Lett.* 86 (5) (2001) 803–806.
- [35] D. Savio, N. Fillot, P. Vergne, H. Hertzler, W. Seemann, G.E.M. Espejel, A multiscale study on the wall slip effect in a ceramic-steel contact with nanometer-thick lubricant film by a nano-to-elastohydrodynamic lubrication approach, *Trans. ASME J. Tribol.* 137 (3) (2015) 031502.
- [36] O. Reynolds, On the theory of lubrication and its application to Mr. Beauchamp Tower's experiments, including an experimental determination of the viscosity of olive oil, *Philos. Trans. R. Soc. Lond.* 177 (1886) 157–234.
- [37] B. Bhushan, Introduction to Tribology, 2nd edition John Wiley & Sons Inc., New York, 2013, 399–409.
- [38] D.J. Evans, G.P. Morriss, Statistical Mechanics of Nonequilibrium Liquids, Academic Press, London, 1990, 77–78.
- [39] L. Bocquet, J.L. Barrat, On the Green-Kubo relationship for the liquid-solid friction coefficient, *J. Chem. Phys.* 139 (4) (2013) 044704.
- [40] L. Bocquet, J.L. Barrat, Flow boundary conditions from nano- to micro-scales, *Soft Matter* 3 (6) (2007) 685–693.
- [41] B.R. Alvarado, S. Kumar, G.P. Peterson, Wettability transparency and the quasiuniversal relationship between hydrodynamic slip and contact angle, *Appl. Phys. Lett.* 108 (7) (2016) 074105.
- [42] L. Bocquet, J.L. Barrat, Hydrodynamic boundary conditions, correlation functions, and kubo relations for confined fluids, *Phys. Rev. E* 49 (4) (1994) 3079–3092.
- [43] H.G. Park, Y.S. Jung, Carbon nanofluidics of rapid water transport for energy applications, *Chem. Soc. Rev.* 43 (2) (2014) 565–576.
- [44] K. Falk, F. Sedlmeier, L. Joly, R.R. Netz, L. Bocquet, Molecular origin of fast water transport in carbon nanotube membranes: Superlubricity versus curvature dependent friction, *Nano Lett.* 10 (10) (2010) 4067–4073.
- [45] K. Falk, F. Sedlmeier, L. Joly, R.R. Netz, L. Bocquet, Ultralow liquid/solid friction in carbon nanotubes: Comprehensive theory for alcohols, alkanes, OMCTS, and water, *Langmuir* 28 (40) (2012) 14261–14272.
- [46] S.K. Kannam, B.D. Todd, J.S. Hansen, P.J. Davis, How fast does water flow in carbon nanotubes, *J. Chem. Phys.* 138 (9) (2013) 094701.
- [47] Y. Demirel, Nonequilibrium Thermodynamics: Transport and Rate Processes in Physical, Chemical and Biological Systems, 3rd edition Elsevier, Amsterdam, 2014 463–464.
- [48] J.B.T. Green, M.T. McDermott, M.D. Porter, Nanometer-scale mapping of chemically distinct domains at well-defined organic interfaces using frictional force microscopy, *J. Phys. Chem.* 99 (1995) 10960–10965.
- [49] A. Berman, C. Drummond, J. Israelachvili, Amontons' law at the molecular level, *Tribol. Lett.* 4 (1998) 95–101.
- [50] Y.S. Leng, S.Y. Jiang, Dynamic simulations of adhesion and friction in chemical force microscopy, *J. Am. Chem. Soc.* 124 (39) (2002) 11764–11770.
- [51] L.Z. Zhang, S.Y. Jiang, Molecular simulation study of nanoscale friction for alkyl monolayers on Si(111), *J. Chem. Phys.* 117 (4) (2002) 1804–1811.
- [52] L.Z. Zhang, L.Y. Li, S.F. Chen, S.Y. Jiang, Measurements of friction and adhesion for alkyl monolayers on Si(111) by scanning force microscopy, *Langmuir* 18 (2002) 5448–5456.
- [53] L.Z. Zhang, S.Y. Jiang, Molecular simulation study of nanoscale friction between alkyl monolayers on Si(111) immersed in solvents, *J. Chem. Phys.* 119 (2) (2003) 765–770.
- [54] L.Z. Zhang, Y.S. Leng, S.Y. Jiang, Tip-based hybrid simulation study of frictional properties of self-assembled monolayers: Effects of chain length, terminal group, scan direction, and scan velocity, *Langmuir* 19 (2003) 9742–9747.
- [55] J.H. Choo, R.P. Glovnea, A.K. Forrest, H.A. Spikes, A low friction bearing based on liquid slip at the wall, *Trans. ASME J. Tribol.* 129 (3) (2007) 611–619.
- [56] M. Kalin, M. Polajnar, The effect of wetting and surface energy on the friction and slip in oil-lubricated contacts, *Tribol. Lett.* 52 (2) (2013) 185–194.
- [57] I.R. Goldian, N. Kampf, A. Yeredor, J. Klein, On the question of whether lubricants fluidize in stick-slip friction, *Proc. Natl. Acad. Sci. U. S. A.* 112 (23) (2015) 7117–7122.
- [58] R.D. Evans, J.D. Cogdell, G.A. Richter, G.L. Doll, Traction of lubricated rolling contacts between thin-film coatings and steel, *Tribol. Trans.* 52 (1) (2008) 106–113.
- [59] Z. Fu, P.L. Wong, F. Guo, Effect of interfacial properties on EHL under pure sliding conditions, *Tribol. Lett.* 49 (1) (2012) 31–38.
- [60] J.Y. Leong, T. Reddyhoff, S.K. Sinha, A.S. Holmes, H.A. Spikes, Hydrodynamic friction reduction in a MAC-hexadecane lubricated MEMS contact, *Tribol. Lett.* 49 (1) (2012) 217–225.
- [61] D. Savio, N. Fillot, P. Vergne, M. Zaccardello, A model for wall slip prediction of confined n-alkanes: Effect of wall-fluid interaction versus fluid resistance, *Tribol. Lett.* 46 (1) (2012) 11–22.
- [62] D.M. Huang, C. Sendner, D. Horinek, R.R. Netz, L. Bocquet, Water slippage versus contact angle: A quasiuniversal relationship, *Phys. Rev. Lett.* 101 (22) (2008) 226101.
- [63] M. Kalin, M. Polajnar, The wetting of steel, DLC coatings, ceramics and polymers with oils and water: The importance and correlations of surface energy, surface tension, contact angle and spreading, *Appl. Surf. Sci.* 293 (2014) 97–108.
- [64] N. Fillot, H. Berro, P. Vergne, From continuous to molecular scale in modelling elastohydrodynamic lubrication: Nanoscale surface slip effects on film thickness and friction, *Tribol. Lett.* 43 (3) (2011) 257–266.
- [65] R. Goldberg, L. Chai, S. Perkin, N. Kampf, J. Klein, Breakdown of hydration repulsion between charged surfaces in aqueous Cs⁺ solutions, *Phys. Chem. Chem. Phys.* 10 (32) (2008) 4939–4945.
- [66] L. Ma, A. Gaisinskaya-Kipnis, N. Kampf, J. Klein, Origins of hydration lubrication, *Nat. Commun.* 6 (2015) 6060.
- [67] U. Raviv, J. Klein, Fluidity of bound hydration layers, *Science* 297 (2002) 1540–1542.
- [68] J. Seror, L.Y. Zhu, R. Goldberg, A.J. Day, J. Klein, Supramolecular synergy in the boundary lubrication of synovial joints, *Nat. Commun.* 6 (2015) 6497.
- [69] C.X. Zhang, Y.H. Liu, S.Z. Wen, S. Wang, Poly(vinylphosphonic acid) (PVPA) on titanium alloy acting as effective cartilage-like superlubricity coatings, *ACS Appl. Mater. Interfaces* 6 (20) (2014) 17571–17578.
- [70] N. Wang, A.M.T. Sfarghiu, D. Portinha, S. Descartes, E. Fleury, Y. Berthier, J.P. Rieu, Nanomechanical and tribological characterization of the mpc phospholipid polymer photografted onto rough polyethylene implants, *Colloids Surf. B: Biointerfaces* 108 (2013) 285–294.
- [71] Y. Ishikawa, T. Sasada, Lubrication properties of hydrogel-coated polyethylene head, *Mater. Trans.* 45 (4) (2004) 1041–1044.
- [72] I. Goldian, S. Jahn, P. Laaksonen, M. Linder, N. Kampf, J. Klein, Modification of interfacial forces by hydrophobin HFBI, *Soft Matter* 9 (44) (2013) 10627.
- [73] D.C. Yue, T.B. Ma, Y.Z. Hu, J. Yeon, A.C.T. van Duin, H. Wang, J.B. Luo, Tribochemistry of phosphoric acid sheared between quartz surfaces: A reactive molecular dynamics study, *J. Phys. Chem. C* 117 (48) (2013) 25604–25614.
- [74] J.J. Li, L. Ma, S.H. Zhang, C.H. Zhang, Y.H. Liu, J.B. Luo, Investigations on the mechanism of superlubricity achieved with phosphoric acid solution by direct observation, *J. Appl. Phys.* 114 (11) (2013) 114901.
- [75] S.A. Whyte, N.J. Mosey, Behavior of two-dimensional hydrogen-bonded networks under shear conditions: A first-principles molecular dynamics study, *J. Phys. Chem. C* 119 (1) (2015) 350–364.
- [76] J.J. Li, C.H. Zhang, L. Ma, Y.H. Liu, J.B. Luo, Superlubricity achieved with mixtures of acids and glycerol, *Langmuir* 29 (1) (2013) 271–275.
- [77] M. Palacio, B. Bhushan, Ultrathin wear-resistant ionic liquid films for novel MEMS/NEMS applications, *Adv. Mater.* 20 (6) (2008) 1194–1198.
- [78] W.J. Zhao, Y. Wang, L.P. Wang, M.W. Bai, Q.J. Xue, Influence of heat treatment on the micro/nano-tribological properties of ultra-thin ionic liquid films on silicon, *Colloids Surf. A Physicochem. Eng. Aspect* 361 (1–3) (2010) 118–125.
- [79] J.B. Pu, D. Jiang, Y.F. Mo, L.P. Wang, Q.J. Xue, Micro/nano-tribological behaviors of crown-type phosphate ionic liquid ultrathin films on self-assembled monolayer modified silicon, *Surf. Coat. Technol.* 205 (20) (2011) 4855–4863.
- [80] J. Sweeney, G.B. Webber, M.W. Rutland, R. Atkin, Effect of ion structure on nanoscale friction in protic ionic liquids, *Phys. Chem. Chem. Phys.* 16 (31) (2014) 16651–16658.
- [81] O.Y. Fajardo, F. Bresme, A.A. Kornyshev, M. Urbakh, Electrotunable lubricity with ionic liquid nanoscale films, *Sci. Rep.* 5 (2015) 7698.
- [82] H. Li, R.J. Wood, M.W. Rutland, R. Atkin, An ionic liquid lubricant enables superlubricity to be “switched on” in situ using an electrical potential, *Chem. Commun.* 50 (33) (2014) 4368–4370.
- [83] A. Gaisinskaya-Kipnis, L. Ma, N. Kampf, J. Klein, Frictional dissipation pathways mediated by hydrated alkali metal ions, *Langmuir* 32 (19) (2016) 4755–4764.

- [84] Y. Xue, Y. Wu, X.W. Pei, H.L. Duan, Q.J. Xue, F. Zhou, How solid-liquid adhesive property regulates liquid slippage on solid surfaces? *Langmuir* 31 (1) (2015) 226–232.
- [85] M. Melillo, F.Q. Zhu, M.A. Snyder, J. Mittal, Water transport through nanotubes with varying interaction strength between tube wall and water, *J. Phys. Chem. Lett.* 2 (23) (2011) 2978–2983.
- [86] I. Moskowitz, M.A. Snyder, J. Mittal, Water transport through functionalized nanotubes with tunable hydrophobicity, *J. Phys. Chem.* 141 (18) (2014) 18C532.
- [87] R.S. Voronov, D.V. Papavassiliou, L.L. Lee, Review of fluid slip over superhydrophobic surfaces and its dependence on the contact angle, *Ind. Eng. Chem. Res.* 47 (8) (2008) 2455–2477.
- [88] T.A. Ho, D.V. Papavassiliou, L.L. Lee, A. Striolo, Liquid water can slip on a hydrophilic surface, *Proc. Natl. Acad. Sci. U. S. A.* 108 (39) (2011) 16170–16175.
- [89] B. Ramos-Alvarado, S. Kumar, G.P. Peterson, Hydrodynamic slip length as a surface property, *Phys. Rev. E* 93 (2) (2016) 023101.
- [90] L. Liu, L. Zhang, Z.G. Sun, G. Xi, Graphene nanoribbon-guided fluid channel: A fast transporter of nanofluids, *Nano* 4 (20) (2012) 6279–6283.
- [91] H. Qiu, X.C. Zeng, W.L. Guo, Water in inhomogeneous nanoconfinement: Coexistence of multilayered liquid and transition to ice nanoribbons, *ACS Nano* 9 (10) (2015) 9877–9884.
- [92] M. Mario, S. Fernandez, M. Neek-Amal, F.M. Peeters, AA-stacked bilayer square ice between graphene layers, *Phys. Rev. B* 92 (24) (2015) 245428.
- [93] A. Verdager, G.M. Sacha, H. Bluhm, M. Salmeron, Molecular structure of water at interfaces: Wetting at the nanometer scale, *Chem. Rev.* 106 (4) (2006) 1478–1510.
- [94] M. Neek-Amal, F.M. Peeters, I.V. Grigorieva, A.K. Geim, Commensurability effects in viscosity of nanoconfined water, *ACS Nano* 10 (3) (2016) 3685–3692.
- [95] T.D. Li, J.P. Gao, R. Szożkiewicz, U. Landman, E. Riedo, Structured and viscous water in subnanometer gaps, *Phys. Rev. B* 75 (11) (2007) 115415.
- [96] R. Renou, A. Szymczyk, G. Maurin, P. Malfreyt, A. Ghofri, Superpermeability of nanoconfined water, *J. Chem. Phys.* 142 (18) (2015) 184706.
- [97] M. Watkins, B. Reischl, A simple approximation for forces exerted on an AFM tip in liquid, *J. Chem. Phys.* 138 (15) (2013) 154703.
- [98] M. Watkins, M.L. Berkowitz, A.L. Shluger, Role of water in atomic resolution AFM in solutions, *Phys. Chem. Chem. Phys.* 13 (27) (2011) 12584–12594.
- [99] J. Hassan, G. Diamantopoulos, D. Homouz, G. Papavassiliou, Water inside carbon nanotubes: Structure and dynamics, *Nanotechnol. Rev.* 5 (3) (2016) 341–354.
- [100] A. Vanossi, N. Manini, M. Urbakh, S. Zapperi, E. Tosatti, Colloquium: Modeling friction: From nanoscale to mesoscale, *Rev. Mod. Phys.* 85 (2) (2013) 529–552.
- [101] Y.D. Zhu, Y. Ruan, Y.M. Zhang, L.H. Lv, X.H. Lu, Nanomaterial-oriented molecular simulations of ion behaviour in aqueous solution under nanoconfinement, *Mol. Simul.* 42 (10) (2016) 784–798.
- [102] Y.D. Zhu, J. Zhou, X.H. Lu, X.J. Guo, L.H. Lv, Molecular simulations on nanoconfined water molecule behaviors for nanoporous material applications, *Microfluid. Nanofluid.* 15 (2) (2013) 191–205.
- [103] J.K. Holt, Methods for probing water at the nanoscale, *Microfluid. Nanofluid.* 5 (4) (2008) 425–442.
- [104] S.H. Zhang, Y.H. Liu, J.B. Luo, In situ observation of the molecular ordering in the lubricating point contact area, *J. Appl. Phys.* 116 (1) (2014), 014302.
- [105] U. Bergmann, Ph. Wernet, P. Glatzel, M. Cavalleri, L.G.M. Pettersson, A. Nilsson, S.P. Cramer, X-ray raman spectroscopy at the oxygen edge of water and ice: Implications on local structure models, *Phys. Rev. B* 66 (9) (2002), 092107.
- [106] A.I. Kolesnikov, J.M. Zanotti, C.K. Loong, P. Thiyagarajan, Anomalously soft dynamics of water in a nanotube: A revelation of nanoscale confinement, *Phys. Rev. Lett.* 93 (3) (2004) 035503.
- [107] M. Plazenet, F. Sacchetti, C. Petrillo, B. Demé, P. Bartolini, R. Torre, Water in a polymeric electrolyte membrane: Sorption/desorption and freezing phenomena, *J. Membr. Sci.* 453 (2014) 419–424.
- [108] J.D. Smith, C.D. Cappa, K.R. Wilson, B.M. Messer, R.C. Cohen, R.J. Saykally, Energetics of hydrogen bond network rearrangements in liquid water, *Science* 306 (29) (2004) 851–853.
- [109] Ph. Wernet, D. Nordlund, U. Bergmann, M. Cavalleri, M. Odelius, H. Ogasawara, L.A. Naslund, T.K. Hirsch, L. Ojamae, P. Glatzel, L.G.M. Pettersson, A. Nilsson, The structure of the first coordination shell in liquid water, *Science* 304 (14) (2004).
- [110] A. Das, S. Jayanthi, H.S.M.V. Deepak, K.V. Ramanathan, A. Kumar, C. Dasgupta, A.K. Sood, Single-file diffusion of confined water inside SWNTs: An NMR study, *ACS Nano* 4 (3) (2010) 1687–1695.
- [111] R. Kolvenbach, L.F. Gonzalez Peña, A. Jentys, J.A. Lercher, Diffusion of mixtures of light alkanes and benzene in nano-sized H-ZSM5, *J. Phys. Chem. C* 118 (16) (2014) 8424–8434.
- [112] X. Liu, X.L. Pan, S.M. Zhang, X.W. Han, X.H. Bao, Diffusion of water inside carbon nanotubes studied by pulsed field gradient NMR spectroscopy, *Langmuir* 30 (27) (2014) 8036–8045.
- [113] C.Y. Ruan, V.A. Lobastov, F. Vigliotti, S. Chen, A.H. Zewail, Ultrafast electron crystallography of interfacial water, *Science* 304 (2004) 80–84.
- [114] S. Belfer, Y. Purinson, R. Fainshtein, Y. Radchenko, O. Kedem, Surface modification of commercial composite polyamide reverse osmosis membranes, *J. Membr. Sci.* 139 (1998) 175–181.
- [115] S.Y. Kwak, D.W. Ihm, Use of atomic force microscopy and solid-state NMR spectroscopy to characterize structure-property-performance correlation in high-flux reverse osmosis (RO) membranes, *J. Membr. Sci.* 158 (1999) 143–153.
- [116] J. Cho, G.A. John Pellegrino, Y. Yoon, Characterization of clean and natural organic matter (NOM) fouled NF and UF membranes, and foulants characterization, *Desalination* 118 (1998) 101–108.
- [117] B. Mi, D.G. Cahill, B.J. Mariñas, Physico-chemical integrity of nanofiltration/reverse osmosis membranes during characterization by Rutherford backscattering spectrometry, *J. Membr. Sci.* 291 (1–2) (2007) 77–85.
- [118] M. Whitby, L. Cagnon, M. Thanou, N. Quirke, Enhanced fluid flow through nanoscale carbon pipes, *Nano Lett.* 8 (9) (2008) 2632–2637.
- [119] Y.D. Zhu, L.Z. Zhang, X.H. Lu, L.H. Lv, X.M. Wu, Flow resistance analysis of nanoconfined water in silt pores by molecular simulations: Effect of pore wall interfacial properties, *Fluid Phase Equilib.* 362 (2014) 235–241.
- [120] L.W. Zhu, P. Attard, C. Neto, Reliable measurements of interfacial slip by colloid probe atomic force microscopy. I. Mathematical modeling, *Langmuir* 27 (11) (2011) 6701–6711.
- [121] L.W. Zhu, P. Attard, C. Neto, Reliable measurements of interfacial slip by colloid probe atomic force microscopy. II. Hydrodynamic force measurements, *Langmuir* 27 (11) (2011) 6712–6719.
- [122] L.W. Zhu, C. Neto, P. Attard, Reliable measurements of interfacial slip by colloid probe atomic force microscopy. III. Shear-rate-dependent slip, *Langmuir* 28 (7) (2012) 3465–3473.
- [123] R. An, Q.M. Yu, L.Z. Zhang, Y.D. Zhu, X.J. Guo, S.Q. Fu, L.C. Li, C.S. Wang, X.M. Wu, C. Liu, X.H. Lu, Simple physical approach to reducing frictional and adhesive forces on a TiO₂ surface via creating heterogeneous nanopores, *Langmuir* 28 (43) (2012) 15270–15277.
- [124] L.L. Zhu, Q. Gu, P.C. Sun, W. Chun, X.L. Wang, G. Xue, Characterization of the mobility and reactivity of water molecules on TiO₂ nanoparticles by ¹H solid-state nuclear magnetic resonance, *ACS Appl. Mater. Interfaces* 5 (20) (2013) 10352–10356.
- [125] K.E. Gubbins, Y. Long, M.S. Bartkowiak, Thermodynamics of confined nano-phases, *J. Chem. Thermodyn.* 74 (2014) 169–183.
- [126] M.S. Bartkowiak, A. Sterczyńska, Y. Long, K.E. Gubbins, Influence of microroughness on the wetting properties of nano-porous silica matrices, *Mol. Phys.* 112 (17) (2014) 2365–2371.
- [127] R. An, L.L. Huang, Y. Long, B. Kalanyan, X.H. Lu, K.E. Gubbins, Liquid-solid nanofriction and interfacial wetting, *Langmuir* 32 (3) (2016) 743–750.